

A High Power Ge n-i-p waveguide photodetector on Silicon-on-Insulator Substrate

Anand Ramaswamy, Nobuhiro Nunoya, Leif A. Johansson and John E. Bowers

Department of Electrical and Computer Engineering, University of California Santa Barbara, Santa Barbara, CA 93106

Matthew N. Sysak and Tao Yin

Intel Corporation, 2200 Mission College Blvd., Santa Clara, CA, 95054, USA

anand@ece.ucsb.edu

Abstract

We demonstrate high current operation of an evanescently coupled Ge waveguide photodetector grown on top of a Si rib waveguide. A $7.4\mu\text{m} \times 500\mu\text{m}$ photodetector was found to dissipate 1.003W of power (125.49mA at -8V).

I. Introduction

Recent efforts to develop photodetectors on a Si platform have centered around high data rate applications where the main focus of device structure and design has been to achieve wide bandwidth operation while simultaneously increasing quantum efficiency and lowering dark current [1, 2]. However, an area that has been relatively less explored is the application of Si based photodetectors to high performance microwave photonic systems. In general, the performance of such systems increases with received shot-noise limited optical power [3]. This necessitates the development of photodiodes that have high optical power handling capability. Surface illuminated InGaAs-InP photodiodes with 199 mA of compression current at a frequency of 1GHz have been reported [4]. Typically, high current operation in a device is limited by 1) space charge effects and 2) thermal effects [5]. It has been shown that space charge effects can be mitigated by appropriate device design [6, 7]. Thermal effects on the other hand are largely a material issue. For example, in surface illuminated InGaAs-InP devices, the thermal conductivity of the InP substrate ($0.68\text{W/cm}\cdot\text{K}$) is a major factor limiting the maximum photocurrent that can be extracted from the device [5]. The problem becomes even more acute for waveguide photodiodes (WG-PD) on an InP platform [8]. This is so because the ternary absorber (usually InGaAs) sits on a quaternary (usually InGaAsP) waveguide. The thermal conductivities of these two layers are $\sim 0.05\text{W/cm}\cdot\text{K}$ [9], which is a factor of 30 less than that of Silicon. Hence, heat flow out of the absorber region is further restricted (compared to a surface illuminated PD) leading to temperature build up and ultimately, thermal failure. For an InP based uni-traveling-carrier (UTC) PD device, failure occurred for a dissipated electrical power of 300mW [10]. An alternate to using an InP substrate is to use Si, because its thermal conductivity ($1.5\text{W/cm}\cdot\text{K}$) is over two times that of InP [9]. Surface illuminated p-i-n detectors made from wafer bonded InGaAs-on-Si material have been reported to dissipate over 612mW of electrical power [11]. In this

work, we present high power operation of a Ge n-i-p waveguide photodetector on silicon-on-insulator (SOI) substrate. The device dissipates 1W of electrical power prior to thermal failure.

II. Device Structure

The Ge waveguide detector is grown on top of a Si rib waveguide by a selective epitaxial process. The detector in this work has a width of $7.4\mu\text{m}$ and a length of $500\mu\text{m}$. The final thickness of the Ge layer is $0.8\mu\text{m}$. The thicknesses of the p^+ silicon and buried oxide layer are $1.5\mu\text{m}$ and $1.0\mu\text{m}$, respectively. The layout of the photodetector and a schematic of the cross section are shown in Figures 1(a) and 1(b).

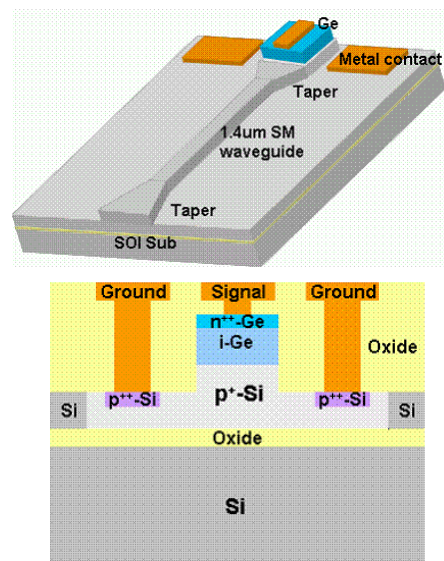


Figure 1 (a): Schematic of Ge detector integrated with passive Si waveguide. (b) Cross-section schematic of device.

As the light propagates along the Si waveguide it evanescently couples upwards into the Ge region where it is absorbed. Details of the growth and fabrication process can be found in [1]. Figure 2 shows a SEM cross-section of the completed device.

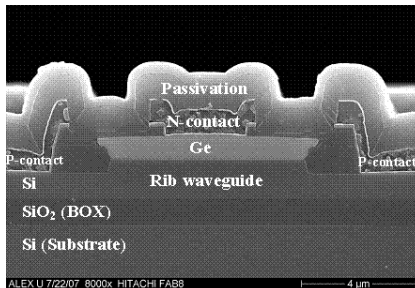


Figure 2: SEM cross-section of a completed device.

III. Experimental Results

Figure 3 (a) shows the saturation characteristics of the device at an input wavelength of 1550nm for different reverse bias values. The x-axis takes into account a coupling loss of 4dB. It can be seen that at a lower bias the output current saturates faster because of carrier screening effects [12]. A maximum photocurrent of 125.49mA under 8V of reverse bias was observed. This corresponds to over 1W of electrical power dissipation in the device.

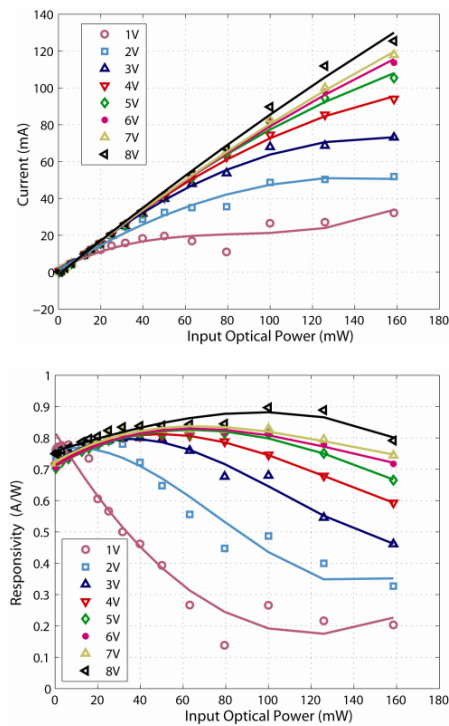


Figure 3 (a): Photocurrent as a function of optical power at different reverse bias voltages (b) dc responsivity as a function of optical power.

Figure 3(b) plots the dc responsivity of the device as a function of input optical power. Typically, at low input optical power levels, the responsivity of a photodiode remains fairly uniform. Close to saturation the photo-generated carriers in the device produce a large screening field that reduces the bias field across the depletion region leading to photocurrent compression. Consequently, the device responsivity is expected to decrease. However, from Figure 3(b) it can be seen that the responsivity is not uniform even at lower optical powers and higher reverse biases (where space charge effects should be minimal). The non-linear behavior of the dc optical responsivity can be attributed to recombination non-linearities [13]. The mechanism for sub-linear recombination events as optical power increases is not fully understood. One possibility [14] is that as the optical power in the depletion (absorber) region increases, the fraction of time that trap sites located at the Ge-Si interface are occupied increases. Consequently, proportionately lower number of minority carriers can recombine as there are fewer available recombination centers (traps).

In addition to dc response measurements, we also measured the frequency response of the device at different photocurrent levels (Figure 4 (a)). It has been observed that the bandwidth of photodiodes decreases at high input optical power levels [15]. However, Figure 4 (b) shows that up to 50mA of photocurrent and under 5V reverse bias, the 3dB bandwidth of the device remains fairly constant at ~4.38GHz.

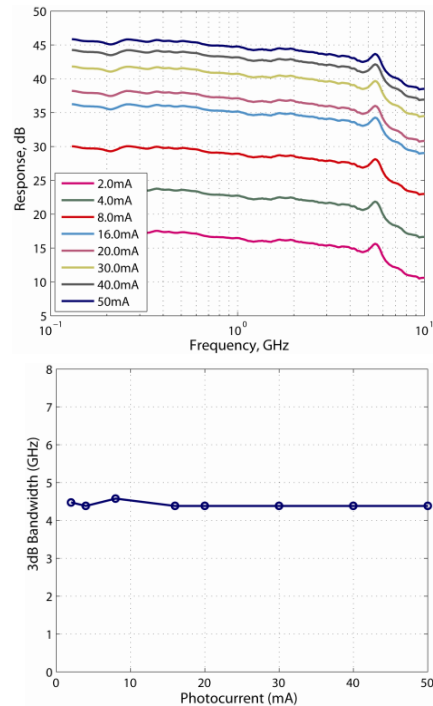


Figure 4(a): Frequency response of 7.4μm X 500μm device at different photocurrent levels for a fixed reverse bias (5V) (b) 3dB bandwidth as a function of photocurrent.

IV. Thermal Simulation

Figure 5 shows the temperature profile from a 2D thermal simulation of the device. The thermal conductivities assumed for Si and Ge are $1.3\text{W/cm}\cdot\text{K}$ and $0.6\text{W/cm}\cdot\text{K}$, respectively. Additionally, the p^{++} Si contacts are assumed to be ideal metal (Al) contacts with a conductivity of $2.37\text{W/cm}\cdot\text{K}$. The absorbed optical power is assumed to generate 124mA of photocurrent and the bias across the device is 8V . As can be seen from the temperature profile in the figure, most of the heat is generated in the absorber region (i-Ge). This heat travels downwards into the p doped Si region and then spreads laterally. The presence of the buried oxide (BOX) layer prevents the heat from being dissipated via the substrate and hence, the temperature builds up in the device. The max temperature (in the absorber) is 85°C when 1W of power is being dissipated across it. An important point to note is that this simulation assumes a uniform absorption profile across the length of the device. However, in reality, the absorption profile of waveguide photodiodes tends to be exponentially decaying. This leads to localized heating and enhanced space charge effects near the input of the waveguide [16].

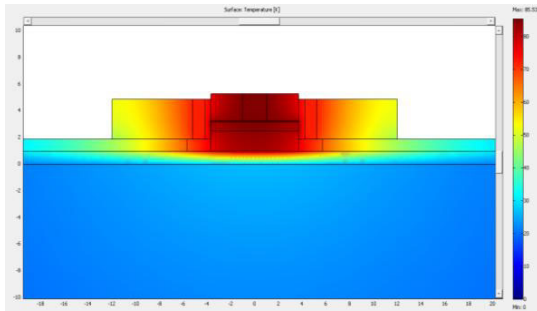


Figure 5: Temperature profile from a 2D thermal simulation of the device.

V. Conclusions

In summary, we have demonstrated high power operation of a Ge n-i-p waveguide photodetector on silicon-on-insulator (SOI) substrate. A $7.4\mu\text{m} \times 500\mu\text{m}$ device was able to dissipate 1W of electrical power. We also measured the frequency response of the device at varying photocurrent levels and found the 3dB bandwidth of the device (4.38GHz) to remain fairly constant even at 50mA of photocurrent. This makes the device attractive for RF photonic applications. Additionally, 2D thermal simulations were performed to determine the heat flow and temperature profile of the device. It was observed that the BOX layer prevented the heat from flowing into the substrate. Instead the heat flows laterally and vertically resulting in higher temperatures in the absorber region.

Acknowledgements

The authors thank K.J. Williams for useful discussions. This research was supported by the DARPA-PHORFRONT program under United States Air Force contract number FA8750-05-C-0265.

References

- [1] T. Yin, *et al.*, "31 GHz Ge n-i-p waveguide photodetectors on Silicon-on-Insulator substrate," *Opt. Exp.*, Vol. 15, Issue 21, pp. 13965-13971, Oct. 2007.
- [2] D. Ahn, *et al.*, "High Performance, waveguide integrated Ge photodetectors," *Opt. Exp.*, Vol 15, Issue 7, pp 3916-3921, Apr. 2007
- [3] V.J. Urick, *et al.*, "Photodiode Linearity Requirements for Radio-Frequency Photonics and Demonstration of Increased Performance using Photodiode Arrays," *Microwave Photonics Conf (MWP)*, Canada Oct. 2008.
- [4] D. A. Tulchinsky *et al.*, "High Saturation Current Wide-Bandwidth Photodetectors," *IEEE J. Select. Topics in Quantum Electron.*, Vol. 10, no. 4, pp. 702 - 708, Aug. 2004.
- [5] K. J. Williams and R. D. Esman, "Design Considerations for High-Current Photodetectors," *J. Lightw. Technol.*, Vol. 17, no. 8, pp. 1443 - 1454, Aug. 1999.
- [6] X. Li *et al.*, "High Saturation current charge compensated InGaAs-InP untraveling-carrier photodiode," *IEEE Photon. Technol. Lett.*, Vol. 15, pp 1276- 1278, Sept. 2003.
- [7] N. Li *et al.*, "High Saturation current InP-InGaAs photodiode with partially depleted absorber," *IEEE Photon. Technol. Lett.*, Vol. 16, pp 864- 866, Mar. 2004.
- [8] J. Klamkin *et al.*, "High Output Saturation and high-linearity untraveling-carrier waveguide photodiodes," *IEEE Photon. Technol. Lett.*, Vol. 19, no. 3, pp 149 - 151, Feb. 2007.
- [9] S. Adachi, "Lattice Thermal Conductivity of Group-IV and III-V Semiconductor Alloys," *J. Appl. Physics.*, vol. 102, no. 6, Sept. 2007.
- [10] J. Klamkin, "Coherent Integrated Receiver for Highly Linear Microwave Photonic Links" *PhD Thesis*, Univ. of California Santa Barbara, Sept. 2008.
- [11] A. Pauchard *et al.*, "Infrared-Sensitive InGaAs-on-Si p-i-n Photodetectors Exhibiting High-Power Linearity," *IEEE Photon. Technol. Lett.*, Vol. 16, no. 11, pp 2544 - 2546, Nov. 2004.
- [12] K. J. Williams, R. D. Esman and M. Dagenais, "Non-linearities in p-i-n microwave photodetectors," *J. Lightw. Technol.*, Vol. 14, no. 1, pp. 84 - 96, Jan. 1996.
- [13] K. J. Williams and R.D. Esman, Klamkin *et al.*, "Photodiode DC and microwave non-linearity at high currents due to carrier recombination non-linearities," *IEEE Photon. Technol. Lett.*, Vol. 10, no. 7 pp 1015 - 1017, Jul. 1998.
- [14] A. R. Schaefer, E. F. Zalewski, and J. Geist, "Silicon detector nonlinearity and related effects," *Appl. Opt.*, vol. 22, no. 8, pp. 1232-1236, Apr. 1983.
- [15] K. J. Williams and R. D. Esman "Observation of photodiode nonlinearities," *Elec. Lett.*, Vol. 28, no. 8, pp. 731 - 732, 1992.
- [16] K.S. Giboney, M. J. W. Rodwell and J. E. Bowers, "Traveling wave photodetector design and measurements," *IEEE J. Select. Topics in Quantum Electron.*, Vol. 2, pp. 622 - 629, Sept. 1996.